Complex Oscillations in the Human Pupil Light Reflex with "Mixed" and Delayed Feedback*

ANDRE LONGTIN
Department of Physics, McGill University, Montreal, Quebec, Canada

AND

JOHN G. MILTON[†]
Department of Neurology, Montreal Neurological Institute, Montreal, Quebec, Canada

ABSTRACT

Simple periodic as well as more complex behaviors are shown to occur in the human pupil light reflex with piecewise constant mixed and delayed feedback. The output of an infrared video pupillometer, an analog voltage proportional to pupil area, is processed by an electronic comparator which synthesizes the piecewise constant feedback. The system is described by a nonlinear delay differential equation which has been previously shown analytically to exhibit periodic and aperiodic behavior. After parameter estimation from the data, it is found that the observed simple periodic behaviors correlate well with the model behaviors. Although more complex behavior can be observed for parameter values which gave complicated dynamics in the model, there is not a one-to-one correspondence between the observed and predicted results. The effect of uncontrollable fluctuations in the parameters on the observability of complex dynamics in this system is discussed.

INTRODUCTION

The control of a physiological variable x is often given by an equation of the form

$$\frac{dx}{dt} \equiv \dot{x} = \text{production} - \text{destruction}$$
$$= g(x(t-\tau)) - \alpha x, \tag{1}$$

where $g(x(t - \tau))$ is a nonlinear function of $x(t - \tau)$ and α is a positive constant [3, 5, 12–15]. The time delay, τ, is an essential feature of these control systems and arises, for example, as the time required for a cell to mature, or the time required for a nerve impulse to travel along an axon and across a synapse, or the time for hormonal signals to travel from their site of production to target organs by diffusion and/or passage through the circulation.

For many physiological control systems, $g(x(t - \tau))$ is a "humped" function of $x(t - \tau)$, i.e., maximal production occurs at some intermediate value of $x(t - \tau)$, and thus the control system displays both positive and negative feedback characteristics [5, 7, 11, 14]. Analytic and computer simulation studies have shown that for various choices of "humped" $g(x(t - \tau))$, Equation (1) can exhibit a rich variety of periodic and aperiodic ("chaotic") dynamics [3, 5, 7, 12]. Moreover, it has been shown that for biologically appropriate choices of $g(t - \tau)$ including estimation of the relevant parameters from published data, there is qualitative agreement between the observed and predicted dynamics [3, 12].

We are not aware of a previous report of an experimental study of the dynamics seen in a physiological control system with delayed mixed feedback. The control of pupil area by the light reflex has been extensively studied as an example of a neurological control system [19–23], and from an experimental point of view, this system offers the advantages that it is readily accessible and can be monitored and manipulated by noninvasive techniques. Here we study a hybrid experimental system for the control of the human pupil light reflex which incorporates piecewise constant delayed and mixed feedback (Figures 1 and 2). For Equation (1) with this kind of
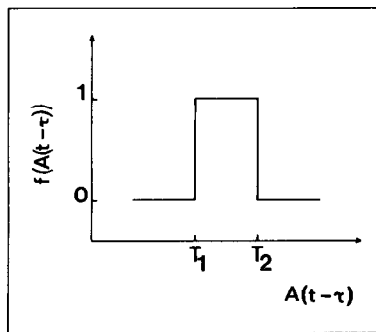

FIG. 1. Piecewise constant delayed-feedback nonlinearity used in this study. The function f is defined in Equation (2). T_1 and T_2 are, respectively, the lower and higher thresholds which are set by the investigator.
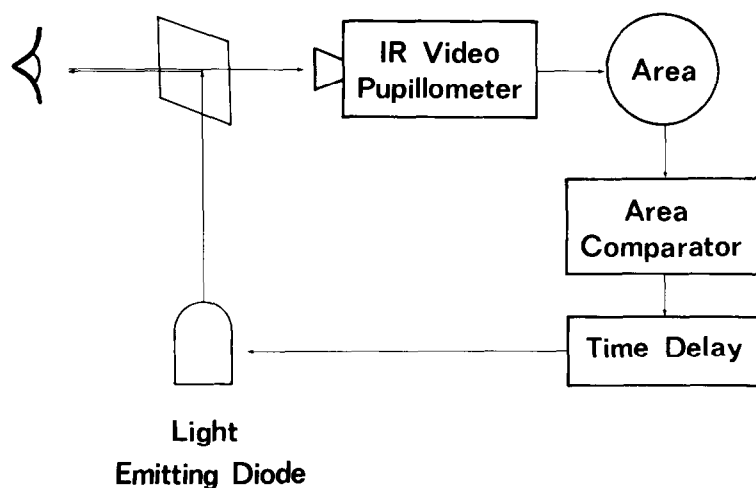
FIG. 2.   Schematic of the instrumentation used for investigating the pupil light reflex with delayed mixed feedback. The area comparator described in "Methods" utilizes operational-amplifier circuitry. Although the Hamamatsu Iriscorder C-2515 is a binocular apparatus, we used it in the monocular mode, as this was more convenient in that only one camera had to be focused and aligned.

feedback, it has been possible to analytically prove the existence of stable equilibria, of stable and unstable limit cycles, and of infinitely many periodic solutions and uncountably many aperiodic, mixing solutions for defined regions in parameter space [6, 7]. With the simple form of the delayed mixed feedback we have chosen, it is possible to compute the solutions exactly and thus to compare the observed and predicted dynamics for different parameter sets. Moreover we are able to quantify the intrinsic variability of certain parameters and thereby address the issue of the observability of complex dynamics in this system.

METHODS

Subjects were healthy males and females ($n = 10$; ages 20–45 years) who were free from both ocular disease and disorders known to affect autonomic function. All measurements were performed in subjects who had been dark adapted for at least 15 minutes in a room lit only by a dim red light. During pupillary measurements, the subjects were instructed to refrain from blinking as much as possible and to fix their gaze on the target appearing on the viewing screen (a dim green asterisk); some subjects performed mental tasks (e.g. multiplication tables) to minimize spontaneous fluctuations in pupil area ("hippus") [1].

Measurements of pupil area were made with an infrared videopupillome-ter (Hamamatsu Binocular Iriscorder C2515) [9]. The video cameras (Figure 2) are of the charge-coupled-device (CCD) type, and their output is analyzed by a frame grabber which counts the number of pixels above a slice level ("gray level") adjusted by the experimenter to discriminate between pupil and iris. The output of the frame grabber is an analog voltage proportional to the pupil area (sampling rate 60 Hz). Light sources were light emitting diodes (peak wavelength of 605 nm). All experiments were done under "open"-loop conditions [23] by focusing a 1.2-mm beam of light on the center of the pupil (initial diameter 5–7 mm). Under these conditions the iris does not alter the beam of light falling on the retina.

The variable x in Equation (1) can be identified with the area of the iris, which is regulated by the autonomic nervous system (parasympathetic and sympathetic), and the function $f(x(t-\tau))$ can be identified with the feed-back of the iris on the light flux to the retina. Since the pupillometer measures pupil area and not iris area, Equation (1) has to be rewritten to take account of the inverse relationship between iris size x and pupil size A. Defining A_0 to be the maximal size of iris plus pupil and $\beta f(A(t-\tau)) = g(A_0 - A(t-\tau))$, we can write $A(t) \approx A_0 - x(t)$, and Equation (1) becomes

$$\dot{A} + \alpha A = -\beta f(A(t-\tau)) - I + \alpha A_0, \qquad (2)$$

where β is the intensity of the light pulse, and α is the reciprocal of the time constant for pupillary movements and is different for constriction (α_c) and dilation (α_d). In going from Equation (1) to Equation (2) we have added a forcing term I to represent the background illumination of the retina. It is important to note that with the choice of $f(A(t-\tau))$ shown in Figure 1, Equation (2) can be solved exactly, without resorting to numerical integra-tion methods, the initial condition being specified by a function defined on the interval $(-\tau, 0)$.

In our experiments the measured pupil area is used to control the timing and duration of light pulses falling on the retina by modifying a technique originally developed by Stark [20]. The control system for the pupil area, given by Equation (2), was constructed by opening the feedback loop and inserting the piecewise constant feedback function (Figure 1) in the follow-ing way. The analog output proportional to the pupil area, A, was compared to the two adjustable thresholds T_1 and T_2 using operational-amplifier circuitry. The output logic level goes HIGH when $T_1 < A < T_2$ and LOW otherwise. The HIGH level drives the light on, and illuminates the retina in open loop. This circuitry is included in Figure 2 as the box labeled "Area Comparator." In our experiments, the pupil being stimulated was also the one being measured.

The solution of Equation (2) requires the specification of seven parame-ters: the time delay; the time constants for constriction and dilation, t_c and

t_d; the asymptotic values the pupil area tends to when the light is ON and OFF, A_{on}, A_{off}; and the lower and upper thresholds, T_1, T_2. The value of A_0 does not affect the qualitative behavior of Equation (2) and was taken to be 100 mm^2. Of the remaining parameters, T_1, T_2 are fixed by the investigator, and the others are estimated experimentally. The neural time delay for the response of the pupil to light was determined as the time between the onset
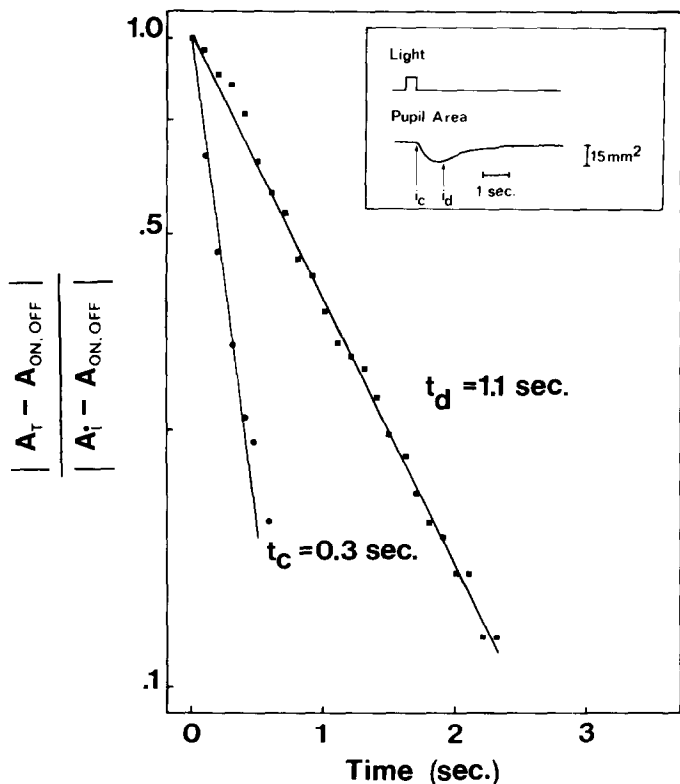

FIG. 3. Plot of the logarithm of the change in pupil area A_t as a function of time following a single 0.5-second light pulse. The changes in pupil area have been normalized to the total change in pupil area that occurs for constriction and dilation respectively. For pupillary constriction the initial value of A_t was measured at the onset of constriction $t = i_c$ (see insert), and the asymptote, A_{on}, was the minimum area obtained with a 2-second light pulse. For pupillary dilation the initial value of A_t was measured at the onset of dilation $t = i_d$. In principle, A_{off} is equal to the initial pupil area (as is true for the example given in the insertion), but typically, following a 0.5-second light pulse the pupil did not dilate back to its initial value suggesting, that some adaptation had occurred. In these cases, A_{off} was reestimated from the time course of the dilation.

of the light pulse and the onset of the pupillary constriction, using a computer program incorporated in the Iriscorder C2515. This neural time delay was assumed to be the same as the time between the cessation of the light pulse and the onset of dilation. The time required for the signal from the video camera to reach the light emitting diode contributed an additional 100-msec delay. The time delay τ in Equation (2) is equal to the neural time delay plus the machine delay. The time constants t_c and t_d were measured as the e^{-1} times for a pupil receiving a single 0.5-second light pulse (Figure 3). The values of the asymptotes are given by

$$A_{\mathrm{on}} = \frac{\alpha_c A_0 - I - \beta}{\alpha_c}, \tag{3}$$

$$A_{\mathrm{off}} = \frac{\alpha_d A_0 - I}{\alpha_d}. \tag{4}$$

The asymptotes were measured as follows: Let A_a be the pupil area at some time when the pupil is constricting; then

$$A_a = A + A_{\mathrm{on}}, \tag{5}$$

where A is a pupil area to be determined. At time $t_c = \alpha_c^{-1}$ later, the pupil area is A_b and we can write

$$A_b = e^{-1}A + A_{\mathrm{on}}. \tag{6}$$

By combining Equations (5) and (6),

$$A = \frac{A_a - A_b}{0.632}, \tag{7}$$

and A_{on} can be calculated from Equation (5). The value of A_{off} can be evaluated in a similar manner when the pupil is dilating.

RESULTS

Figure 3 (insert) shows the change in pupil diameter as a function of time following a single 0.5-second light pulse. After a delay of 292 ± 10 msec (mean $\pm$ SD for 10 subjects), the pupil undergoes a rapid constriction followed by a slower dilation. The time courses for constriction and dilation are both reasonably well fitted by a single exponential decay: $t_c = 0.4 \pm 0.1$ seconds; $t_d = 1.4 \pm 0.4$ seconds for 5 subjects. These observations suggest that for the hybrid system incorporating the choice of $f(A(t - \tau))$ shown in Figure 1, Equation (2) will provide a good description of the response of the pupil to light.
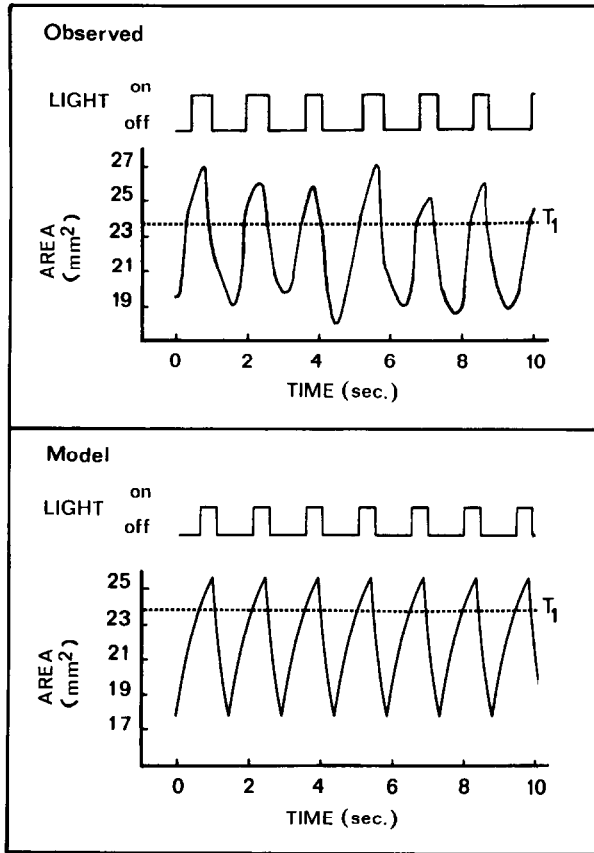
FIG. 4. Example of pupil cycling in a one-threshold experiment (case 1). Simple periodic behavior (referred to as type 1 in Figure 5) is initiated at the left by lowering T_1 to the level indicated. Above the data, we have shown the sequence of light pulses seen by the retina. In the experiment (top graph) the light turns on (off) 100 msec after the pupil area crosses the threshold area T_1. This time delay represents the machine delay. The model solution was obtained by using the following parameters: $\tau = 0.385$ sec, $\alpha_c = 2.50$ sec^{-1}, $\alpha_d = 1.25$ sec^{-1}, $A_{on} = 14.2$ mm^2, $A_{off} = 28.7$ mm^2, $T_1 = 23.8$ mm^2, $T_2 = 70.0$ mm^2. The values of A_{on}, A_{off} represent the average of the values obtained for each cycle (see Figure 8). Initial pupil area is 34 mm^2.

CASE 1: $A_{on} < T_1 < A_{off} < T_2$

Figure 4 shows the behavior of pupil area when the lower threshold T_1 is chosen to be between the asymptotes and also the upper threshold T_2 is greater than the upper asymptote A_{off}. Under these conditions, pupil area undergoes repetitive constrictions and dilations, the light being turned on whenever the pupil area A is greater than T_1. The period of these oscillations

is the time between successive pupillary constrictions and is a function of the values of A_{on}, A_{off}, the time constants, and the total time delay τ (the intrinsic neural time plus that of the electronic feedback). The mean period of pupil cycling can be varied from 1 to 8 seconds by changing T_1 and τ (data not shown). We have found that the observed mean period over this range agrees with that predicted by Equation (2) to within 20% (typically better than 10%) (Longtin and Milton, in preparation).

CASE 2: $A_{on} < T_1 < T_2 < A_{off}$

Figure 5 gives a representative bifurcation diagram for the calculated solution of Equation (2) over the parameter space spanned by (T_1, T_2). Our computer simulations indicate that for the delay present in the system (380–450 msec), most regions of this subspace correspond to stable periodic behavior; however, in a narrow band (labeled C in Figure 5) solutions of
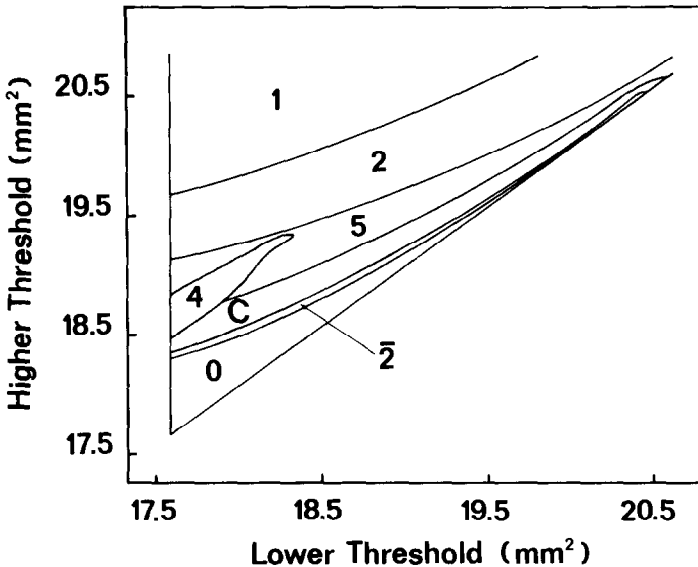

FIG. 5. Dynamic picture in a region of parameter space spanned by the thresholds T_1 and T_2 (note that $T_1 < T_2$). The numbers labeling the different regions correspond to the number of light pulses per period in the exact solutions of Equation (2). Only the low-periodicity regions are indicated. All of the more complicated solutions belong to the region marked C. Note that the solution in the narrow region marked $\bar{2}$ is qualitatively different from the one marked 2. Parameter values are $\tau = 0.425$ sec, $\alpha_c = 4.00$ sec^{-1}, $\alpha_d = 1.429$ sec^{-1}, $A_{on} = 15.0$ mm^2, $A_{off} = 22.0$ mm^2.

different periodicities are in close proximity and aperiodic ("chaotic") solutions occur. For simplicity we have represented the dynamics by the number of light pulses per periodic cycle. Although the solutions within each region have the same qualitative features, i.e. number of light pulses per period, they do not necessarily have the same period. The region labeled 0 corresponds to solutions where the pupil area dilates asymptotically to A_{off}. The region labeled 1 corresponds to results of the type shown in Figure 4, i.e. one light pulse per cycle.

Next to region 1 is a region labeled 2, corresponding to two light pulses per cycle. Figure 6 compares the observed and predicted dynamics for a
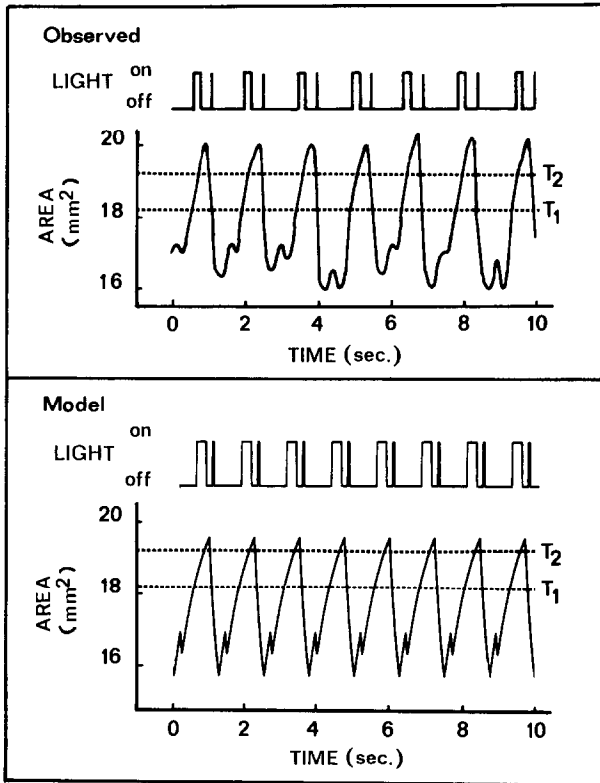

FIG. 6. Example of a solution characteristic of region 2, in which the retina sees a double pulse of light in each cycle. The model prediction is given in the lower half of the figure. Parameter values are $\tau = 0.425$ sec, $\alpha_c = 4.00$ sec^{-1}, $\alpha_d = 1.429$ sec^{-1}, $T_1 = 18.2$ mm^2, $T_2 = 19.2$ mm^2, $A_{on} = 13.8$ mm^2, $A_{off} = 21.3$ mm^2. The averaged values of the asymptotes were determined as in Figure 4.

choice of T_1 and T_2 within this region. For solutions of this type a smaller
pupillary constriction-dilation change occurs in the trough of the larger one.
As for the dynamics observed in region 1, there is good agreement between
theory and experiment. It should be noted that the transition $1 \rightarrow 2$ corre-
sponds to a bifurcation in Equation (2), but that it is not a period-doubling
bifurcation, since little change in period occurs. There is also another region
in which there are two light pulses per cycle, labeled as $\bar{2}$. Solutions in this
region have the smaller pupillary constriction-dilation change occurring on
the peak of the larger one. We have not observed solutions of this type.

Close to region 2 there are smaller regions containing more complex
dynamics, i.e. regions 4, 5, and C. The period varies continuously in each of
these regions. The boundary between regions 2 and 5 corresponds to a
period-doubling bifurcation, but the boundary between regions 4 and 5 does
not. Additional period doublings have been shown to occur in region C.

In Figure 7 we show the observed oscillations in pupil area in an
experiment in which the lower threshold T_1 was held constant and the upper
threshold T_2 was adjusted to a value which produces a region-5 solution of
Equation (2). With this choice of T_1 and T_2 more complex oscillations are
obtained than were observed in region 2 [compare Figures 6 and 7(b)].
Figure 7(c) shows the solution of Equation (2) for the parameters estimated
from the data in Figure 7(b). Although there is not a one-to-one correspon-
dence between the observed and predicted oscillations, there are nonetheless
some similarities. The region-5 solution shows a recurring pattern of a large
pupil dilation-constriction, followed by a smaller one, then another larger
one followed by two smaller ones. A similar pattern in the successive
amplitudes is seen during the first 7 seconds of the observed oscillation
[Figure 7(b)]. The period of this recurrence in the successive amplitudes of
the observed oscillations over the first seven seconds is ≈ 3.6 seconds, which
is ≈ 2.2 times the period of the corresponding region-1 oscillation shown in
Figure 7(a). This observation offers support for the possibility that the
observed oscillation is, at least transiently, in a region of parameter space
associated with a period doubling, i.e. region 5, or more complex.

We next explored the solutions of Equation (2) in the neighborhood of
the region-5 solution shown in Figure (7c) to see if better agreement with the
observed oscillation could be obtained. Figure 7(d) shows a solution of
Equation (2) which is closer to the observed oscillation over the first 7
seconds. This solution was obtained by increasing the parameter A_{off} by
only 5%. The period of this solution is ≈ 2.1 times that of the corresponding
region-1 solution (i.e. the solution with the same T_1). These observations
emphasize the sensitivity of the solutions of Equation (2) to small fluctua-
tions in the control parameters.

Even more complicated oscillations are observed when the thresholds are
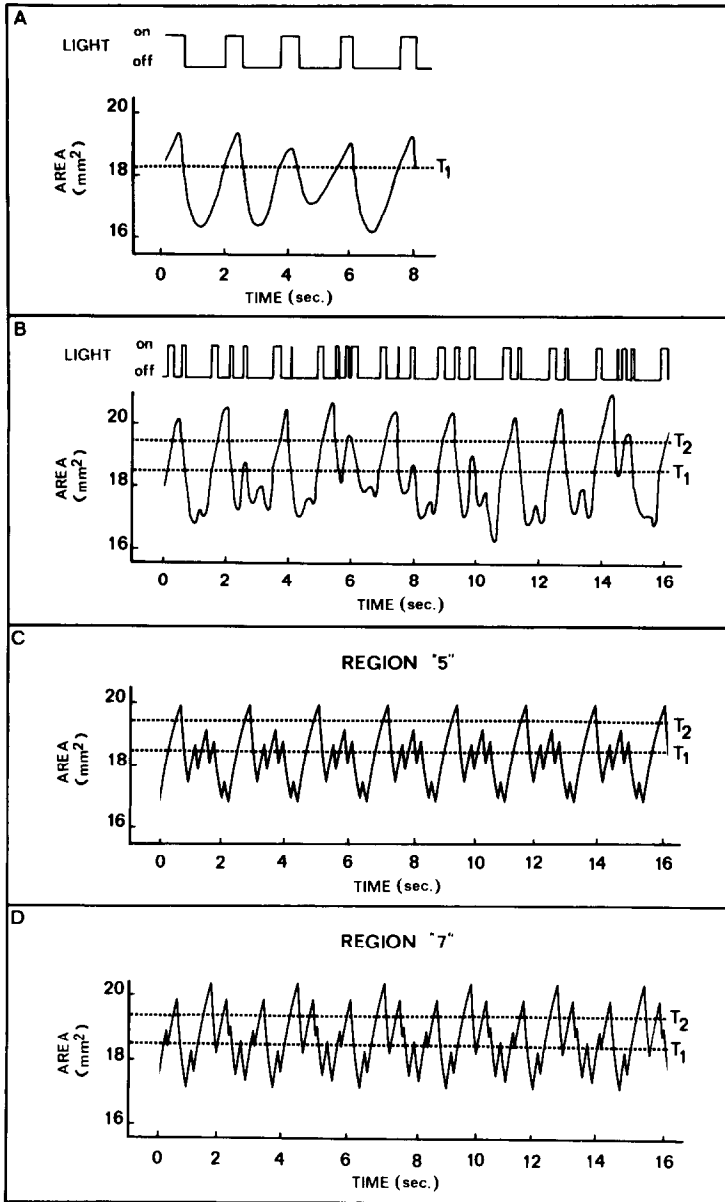chosen to give solutions in region C (data not shown).

FIG. 7. Experimentally observed pupil oscillations near a period-doubling bifurcation. (a) shows the pupil oscillation obtained when $T_1 = 18.5$ mm^2 and $T_2 = 40$ mm^2, and (b) shows the oscillation obtained when T_2 is lowered to 19.5 mm^2 and T_1 is held constant. (c) shows the solution of Equation (2) for the parameters estimated from (b): $\tau = 0.425$ sec, $\alpha_c = 4.0$ sec^{-1}, $\alpha_d = 1.429$ sec^{-1}, $A_{on} = 16.0$ mm^2, $A_{off} = 22.0$ mm^2. (d) shows a solution of Equation (2) using the same parameters as used for (c) except that A_{off} was increased to 23.05 mm^2.

"NOISE" AND OBSERVABILITY

It is possible that the lack of agreement between the solutions of Equation (2) and the observed complex oscillations [compare Figure 7(b) and (c)] may have arisen because of uncontrollable fluctuations in certain of the control parameters describing the pupil's response to light [compare Figure 7(c) and (d)]. Here we examine this possibility.

We assumed that the only parameters that changed in our experiments were the values of the asymptotes (see Methods and Discussion). Support for this assumption is given in Figure 8. In Figure 8(b) we plot the values of the asymptotes as a function of the ith cycle for the data shown in Figure 4, and in Figure 8(a) we compare the measured period for each cycle with the period predicted from Equation (2) using the corresponding values of
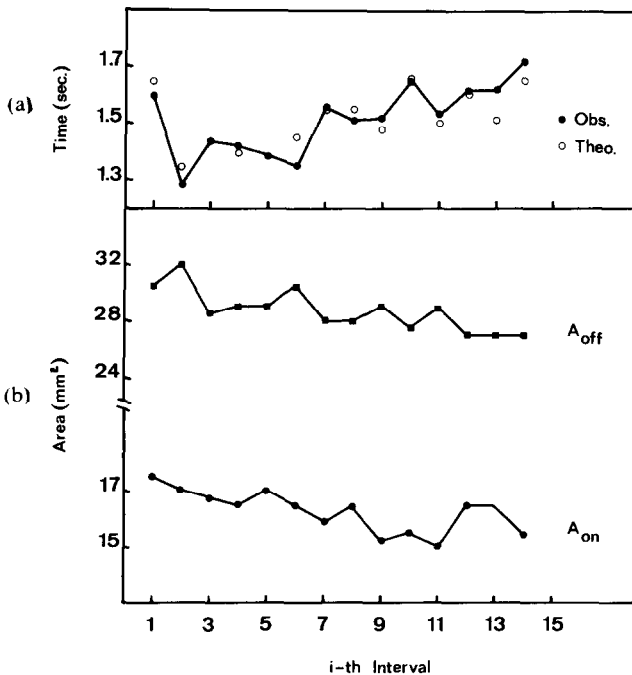

FIG. 8. (a) Comparison of the measured (●) and predicted (○) cycle times for the data given in Figure 4. (b) The predicted cycle times have been calculated from Equation (2) using the appropriate values of the asymptotes and represent the steady-state period. The estimated error in the asymptotes was 0.5 mm².
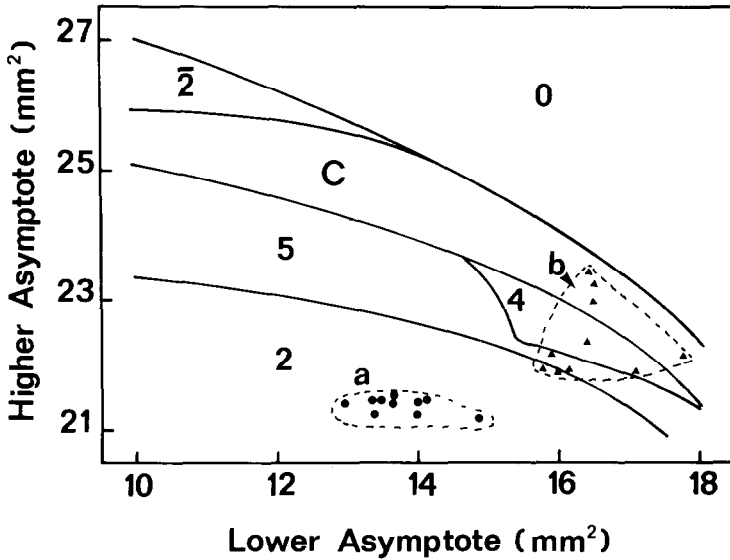
FIG. 9. Dynamical picture in a region of parameter space spanned by the asymptotes A_{on} and A_{off}. The labeling is the same as in Figure 5. Parameter values are $\tau = 0.425$ sec, $\alpha_c = 4.00$ sec^{-1}, $\alpha_d = 1.429$ sec^{-1}. The values of the asymptotes in the region labeled a ($\bullet$) were measured for the oscillation shown in Figure 6, and those in the region labeled b ($\blacktriangle$) have been measured for the oscillations shown in Figure 7(b). The dynamic pictures for a and b were sufficiently close to warrant the use of the same diagram to display the variability of the asymptotes. The estimated error in measuring the asymptotes was 0.5 mm^2.

the asymptotes. In this manner it can be seen that the variations in period are largely accounted for by the variations in the asymptotes.

Figure 9 shows a region of parameter space spanned by (A_{on}, A_{off}) in which T_1 and T_2 are fixed at the values used to obtain the type-2 oscillations shown in Figure 6 and the oscillations in Figure 7. In this parameter space, we have plotted the measured values for the asymptotes for each successive cycle for these oscillations—respectively, area a and area b. It is clear that our ability to observe oscillations which resemble the type-2 solutions of Equation (2) is due to the fact that the variations in the asymptotes are not large enough to go outside region 2 in parameter space. On the other hand, it is not surprising that we were not able to obtain agreement between our model and the observations in Figure 7(b), since the fluctuations in the values of the asymptotes overlap several regions in this parameter space. Presumably the experimentally observed oscillations shown in Figure 7(b)

represent a mixture of solutions from these adjacent regions in parameter space and transients.

DISCUSSION

We have studied the dynamics of a hybrid system for the control of the human pupil light reflex possessing mixed delayed feedback, and compared the observed with the predicted dynamics. The piecewise constant delayed mixed feedback function shown in Figure 1 was chosen because it has the advantage of being well characterized analytically [6–7], all the relevant parameters can be directly estimated from the experimental data, and the corresponding solutions of the model can be computed exactly. It must be emphasized that the solutions of this model [i.e. the solutions of Equation (2)] are solutions of an autonomous delay differential equation and not the response to external periodic forcing.

We observed a rich variety of dynamics, including no oscillation (region 0), simple limit-cycle oscillations (regions 1 and 2), and more complex oscillations [Figure 7(b)]. There was quantitative agreement between the observed oscillations and those predicted by Equation (2) in region 1, and good qualitative agreement with the model in region 2. The model also correctly predicted the parameter ranges over which more complicated dynamics are observed experimentally.

However, for the more complex oscillations there is not good agreement between the observed pupillary dynamics and those predicted by Equation (2). We suggest that these discrepancies arise because of unmodeled fluctuations in certain of the parameters which describe the pupil's response to light. As the oscillations become more and more complicated in the model, the corresponding regions in parameter space become smaller and smaller (see Figures 5 and 9). Eventually the region in parameter space occupied by the variability of these parameters becomes large relative to the size of the region over which a particular type of oscillation occurs. This is reflected experimentally by a solution which combines the dynamics observed in neighboring regions of parameter space as well as transients [solutions of Equation (2) often show long transients before settling on a periodic cycle]. Although in other physiological [4] and physical [2, 10, 18, 24] systems it has been possible to observe more bifurcations than we observe here, the inherent noise in the system eventually prevents the observation of the predicted dynamics [8, 17].

There are five parameters in Equation (2) which can undergo changes in our experiments: the time delay (τ), the rate constants for constriction and dilation (α_c, α_d), and the asymptotes (A_{on}, A_{off}). We assume that the only parameters which changed in our experiments were the values of the asymptotes. The main rationale for this assumption is the observation that it

permitted good agreement between experiment and theory for the region-1 and -2 solutions with all values of the parameters being measured from the data (Figures 4 and 6). In contrast, when we assumed that the only parameters which changed were the values of the rate constants, there was no agreement between the model and any of the observed oscillations. Finally, computations showed that the observed variations in the intrinsic neural delay (± 30 msec) were not large enough to significantly influence the predicted dynamics. Although these observations do not eliminate the possibility that these latter parameters have also changed during our experiments, they do suggest that the most significant changes in the parameters affecting the dynamical behavior of our system occur in the asymptotes.

There are a number of factors which contribute to the changes in the values of the asymptotes. A major influence is the adaptation of the retina to the average light level (ambient light plus the repetitive light pulses during pupil cycling) [19–20]. As the pupil cycle time is decreased from 7 to 1 seconds, the fraction of time that the light is on increases from 0.01 to 0.40 (data not shown). Thus under conditions of more rapid cycling the pupil will tend to be smaller (since the average light level is greater). In addition, there are other retinal factors such as photoreceptor bleaching, as well as the influence of other neural systems on the pupil light reflex such as the ascending reticular activating system (occurring in particular at the level of the Edinger-Westphal nucleus), the accommodation reflex, and the resting activity of the optic nerve [16].

It is possible that by constructing a model incorporating all of the influences on the values of the asymptotes, it might be possible to predict the observed dynamics in more detail. In particular, extension of our model to at least a second-order delay differential equation would be required to eliminate the slope discontinuities present in Equation (2). However, besides rendering the exact computation of orbits and estimation of relevant parameters more difficult, we expect that as the predicted dynamics become more complex, the region in parameter space over which they are observed will become narrower until the remaining "unmodeled" noise becomes larger than these regions, thus rendering the dynamics unobservable. Although it is clear that such an approach would narrow the region in this extended parameter space over which unmodeled parameter variability occurs, it remains to be seen whether this narrowing would be great enough to allow observation of the more complex predicted dynamics.

"Noisy" variations are characteristically seen in physiological data. The fact that Equation (1) can admit very complicated dynamics suggests the possibility that some of this noise may be of deterministic origin [3, 7, 12, 15]. However, it is clear that in any real physical or biological system there will also be some degree of stochasticity, for example in the form of thermal noise, and that deterministic chaos, if present at all, will be superposed on

this background signal. In our system, complicated "noisy" solutions are observed even for parameter choices which do not correspond to chaotic solutions of Equation (2). We feel that these noisy behaviors reflect a combination of different types of solutions in adjacent regions of parameter space and transients resulting from the perturbations introduced by the noisy parameters.

REFERENCES

1   J. H. Bouma and L. C. J. Baghuis, Hippus of the pupil: Periods of slow oscillations of unknown origin. *Vision Res.* 11:1345–1351 (1971).
2   H. M. Gibbs, F. A. Hopf, D. L. Kapana, and R. L. Shoemaker, Observation of chaos in optical bistability, *Phys. Rev. Lett.* 46:474–477 (1981).
3   L. Glass and M. C. Mackey, Pathological conditions resulting from instabilities in physiological control systems, *Ann. N.Y. Acad. Sci.* 316:214–235 (1979).
4   M. R. Guevara, L. Glass, and A. Shrier, Phase locking, period-doubling bifurcations, and irregular dynamics in periodically stimulated cardiac cells, *Science* 214:1350–1353 (1981).
5   U. an der Heiden, Delays in physiological systems, *J. Math. Biol.* 8:345–364 (1979).
6   U. an der Heiden, Stochastic properties of simple differential-delay equations, in *Delay Equations: Approximation and Application* (G. Meinardus and G. Nurnberger, Eds.), ISNM Series, Birkhäuser, Boston, 1985.
7   U. an der Heiden and M. C. Mackey, The dynamics of production and destruction: Analytic insight into complex behaviour, *J. Math. Biol.* 16:75–101 (1982).
8   W. Horsthemke and D. K. Kondepudi (Eds.), *Fluctuations and Sensitivity in Nonequilibrium Systems*, Springer, New York, 1984.
9   S. Ishikawa, M. Naito, and K. Inaba, A new videopupillography, *Ophthalmologica* 160:248–259 (1970).
10   A. Libchaber, C. Laroche, and S. Fauve, Period doubling cascade in mercury, a quantitative measurement, *Phys. Lett.* 43:L211–L216 (1982).
11   N. MacDonald, *Time Lags in Biological Models*, Springer, New York, 1978.
12   M. C. Mackey and L. Glass, Oscillation and chaos in physiological control systems, *Science* 197:287–289 (1977).

13 M. C. Mackey and U. an der Heiden, Dynamical diseases and bifurcations: Under-
    standing functional disorders in physiological systems, *Funkt. Biol. Med.* 1:156–164
    (1982).

14 M. C. Mackey and U. an der Heiden, The dynamics of recurrent inhibition, *J. Math.
    Biol.* 19:211–225 (1984).

15 M. C. Mackey and J. G. Milton, Dynamical diseases, *Ann. N.Y. Acad. Sci.* 504:16–32
    (1987).

16 N. R. Miller (Ed.), *Walsh and Hoyt's Clinical Neuro-Ophthalmology*, Vol. 2, 1985, pp.
    400–441.

17 R. M. Noyes, The interface between mathematical chaos and experimental chemistry,
    in *Stochastic Phenomena and Chaotic Behaviour in Complex Systems* (P. Schuster, Ed.),
    1984, pp. 106–115.

18 R. H. Simoyi, A. Wolf, and H. L. Swinney, One-dimensional dynamics in a multicom-
    ponent chemical reaction, *Phys. Rev. Lett.* 49:245–248 (1982).

19 L. Stark, Stability, oscillations and noise in the human pupil servomechanism, *Proc.
    Inst. Radio Engrs.* IRE 47:1925–1939 (1959).

20 L. Stark, Environmental clamping of biological systems: Pupil servomechanism, *J.
    Opt. Soc. Amer.* 52:925–930 (1962).

21 L. Stark, *Neurological Control Systems: Studies in Bioengineering*, Plenum, New York,
    1969.

22 L. Stark, The pupil as a paradigm for neurological control systems, *IEEE Trans.
    Biomed. Engrg.* BME-31:919–924 (1984).

23 L. Stark and P. M. Sherman, A servoanalytic study of consensual pupil reflex to light,
    J. Neurophys. 20:17–26 (1957).

24 R. Vallee, C. Delisle, and J. Chrostowski, Noise versus chaos in acousto-optic
    bistability, *Phys. Rev. A* 30:336–344 (1984).